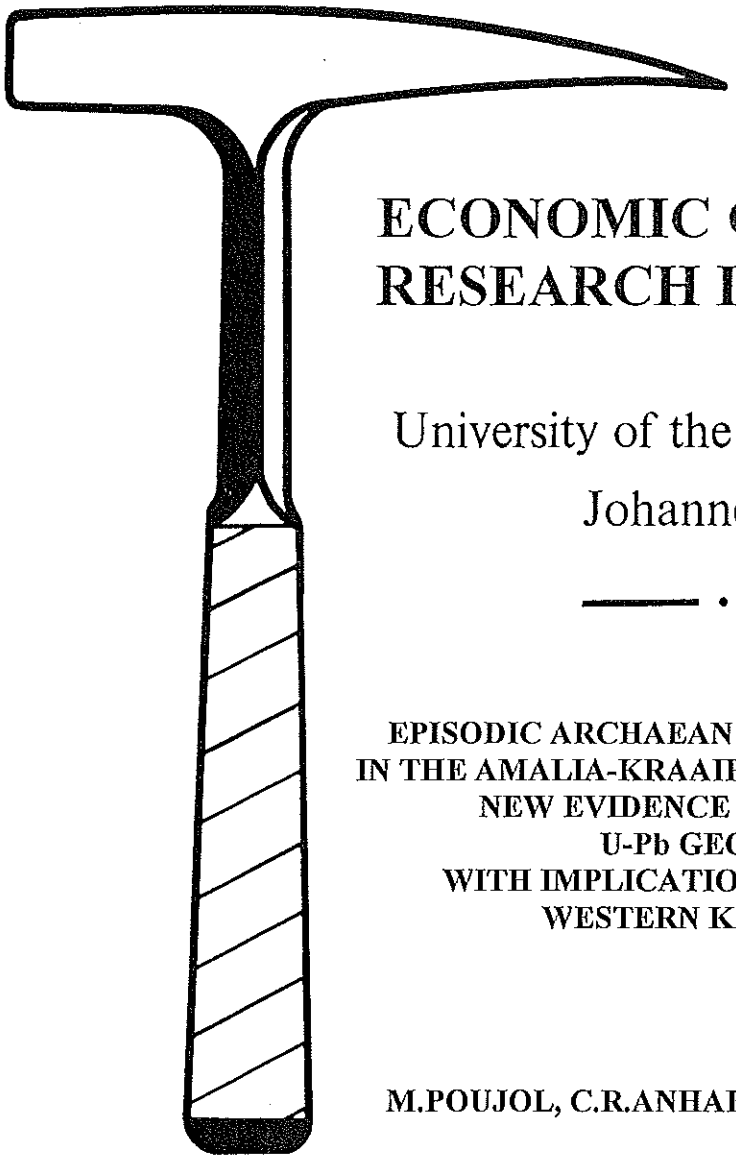

ECONOMIC GEOLOGY RESEARCH INSTITUTE

University of the Witwatersrand

Johannesburg

EPISODIC ARCHAEAN GRANITOID EMPLACEMENT IN THE AMALIA-KRAAIPAN TERRANE, SOUTH AFRICA: NEW EVIDENCE FROM SINGLE ZIRCON U-Pb GEOCHRONOLOGY WITH IMPLICATIONS FOR THE AGE OF THE WESTERN KAAPVAAL CRATON

M.POUJOL, C.R.ANHAEUSSER and R.A.ARMSTRONG

INFORMATION CIRCULAR No. 346

UNIVERSITY OF THE WITWATERSRAND
JOHANNESBURG

EPISODIC ARCHAEAN GRANITOID EMPLACEMENT IN THE AMALIA-KRAAIPAN TERRANE, SOUTH AFRICA: NEW EVIDENCE FROM SINGLE ZIRCON U-Pb GEOCHRONOLOGY WITH IMPLICATIONS FOR THE AGE OF THE WESTERN KAAPVAAL CRATON

by

M. POUJOL[1], C.R. ANHAEUSSER[2], AND R.A. ARMSTRONG[3]

([1]Hugh Allsopp Laboratory/ Economic Geology Research Institute, Private Bag 3, University of the Witwatersrand, WITS 2050, South Africa
[2]Economic Geology Research Institute, Private Bag 3, University of the Witwatersrand, WITS 2050, South Africa
[3]Research School for Earth Sciences, The Australian National University, Canberra, ACT 0200, Australia)

ECONOMIC GEOLOGY RESEARCH INSTITUTE
INFORMATION CIRCULAR No. 346

August, 2000

EPISODIC ARCHAEAN GRANITOID EMPLACEMENT IN THE AMALIA-KRAAIPAN TERRANE, SOUTH AFRICA: NEW EVIDENCE FROM SINGLE ZIRCON U-Pb GEOCHRONOLOGY WITH IMPLICATIONS FOR THE AGE OF THE WESTERN KAAPVAAL CRATON

ABSTRACT

The Amalia-Kraaipan granite-greenstone terrane, located in the western part of the Kaapvaal Craton, consists of metamorphosed mafic volcanic rocks and interlayered ferruginous and siliceous metasediments, together with a variety of granitoid rocks, the latter comprising tonalitic and trondhjemitic gneisses, granodiorites and adamellites. This study presents new single zircon dating for a variety of granitoid occurrences from both the Amalia and Kraaipan terranes.

The new U-Pb data demonstrate episodic granitoid emplacement events, which occurred over a time-span of approximately 220 Ma in the Amalia-Kraaipan terrane. The oldest granitoid rocks thus far recognised, and which have been dated at *c.* 3008 Ma, are represented by biotite-trondhjemite gneisses located southwest of the town of Amalia. Homogeneous leuco-trondhjemite dykes intruding these gneisses have yielded an age of *c.* 2940 Ma. Two granodiorite samples from the central part of the Amalia-Kraaipan terrane were dated at 2913 ± 17 Ma and 2915 ± 12 Ma, respectively, while a further two granodiorite samples from both the central and northern parts of the study area were dated at 2879 ± 9 Ma and 2879 ± 11 Ma. The youngest granitoid body, the Mosita adamellite, which is exposed in the northwest sector of the Amalia-Kraaipan terrane, yielded an age of 2791 ± 8 Ma.

As the biotite-trondhjemite gneisses, which contain conformably interlayered amphibolite xenoliths, are now shown to be *c.* 3008 Ma years old in the Amalia region, the Kraaipan Group volcano-sedimentary rocks developed in this area are therefore regarded as being older than 3008 Ma. The Witwatersrand Basin, the western edge of which is developed approximately 60km east of the Amalia-Kraaipan terrane, is reported elsewhere as having been deposited between 3074 and 2714 Ma. The 3010 to 2920 Ma Amalia-Kraaipan granitoids described in this paper could, therefore, represent a possible source for some of the Witwatersrand sediments and their contained gold mineralization. Lastly, the *c.* 2791 Ma age obtained for the Mosita adamellite suggests that there may be a possible genetic link between this granitoid body and the *c.* 2781 Ma Gaborone Granite Suite and the associated volcanic rocks of the Kanye Formation exposed approximately 120 km to the north in neighbouring Botswana.

oOo

EPISODIC ARCHAEAN GRANITOID EMPLACEMENT IN THE AMALIA-KRAAIPAN TERRANE, SOUTH AFRICA: NEW EVIDENCE FROM SINGLE ZIRCON U-Pb GEOCHRONOLOGY WITH IMPLICATIONS FOR THE AGE OF THE WESTERN KAAPVAAL CRATON

CONTENTS

	Page
INTRODUCTION	1
GENERAL GEOLOGY	3
PREVIOUS GEOCHRONOLOGICAL INVESTIGATIONS	4
Sampling	6
ANALYTICAL TECHNIQUES	7
U-Th-Pb SHRIMP I and II Analyses	8
U-Pb Conventional Single Zircon Technique	8
RESULTS AND INTERPRETATIONS	8
Trondhjemitic Granitoid Samples	8
Granodiorites and Adamellites	14
CONCLUSIONS	17
REFERENCES	18

oOo

Published by the Economic Geology Research Institute
Department of Geology
University of the Witwatersrand
1 Jan Smuts Avenue
Johannesburg 2001
South Africa
www.wits.ac.za/egru

ISBN 1-86838-290-7

EPISODIC ARCHAEAN GRANITOID EMPLACEMENT IN THE AMALIA-KRAAIPAN TERRANE, SOUTH AFRICA: NEW EVIDENCE FROM SINGLE ZIRCON U-Pb GEOCHRONOLOGY WITH IMPLICATIONS FOR THE AGE OF THE WESTERN KAAPVAAL CRATON

INTRODUCTION

The Amalia-Kraaipan granite-greenstone terrane (Fig 1), located in the western part of the Kaapvaal Craton, consists of metamorphosed mafic volcanic rocks, interlayered ferruginous and siliceous metasediments (mainly banded iron formations and cherts) and granitoids rocks, including tonalitic and trondhjemitic gneisses (TTG), granodiorites and adamellites (Anhaeusser and Walraven, 1999). This terrane is poorly exposed beneath cover sequences comprising mainly Neoarchaean Ventersdorp Supergroup volcanic rocks and a blanket of Tertiary to Recent Kalahari sediments.

Because of poor exposures in the central and western parts of the Kaapvaal Craton, most of the information on the basement rocks has been derived from the eastern and northern sectors. Good exposures are also found in places on the Johannesburg Dome, in the central Kaapvaal Craton (Anhaeusser, 1973; 1999; Anhaeusser and Burger, 1982; Poujol and Anhaeusser, 1999), and in areas to the southwest where granitic basement inliers occur, extending from west of Johannesburg towards Schweizer-Reneke (Klemd and Hallbauer, 1987; Robb and Meyer, 1990; Drennan et al., 1990). Additional information on the nature of the granitic basement is available from boreholes drilled by mining companies seeking extensions to gold mineralization in the Witwatersrand Basin (Klemd and Hallbauer, 1987; Robb et al., 1990; Drennan et al., 1990; Robb et al., 1992).

Further to the west, in the Mafikeng-Vryburg area (Fig.1), very few outcrops of granitoid rocks have been reported. Where exposed these are generally weathered and poorly preserved (Keyser and Du Plessis, 1993; Liebenberg, 1977; Michaluk and Moen, 1991; Schutte, 1994; Van Eeden et al., 1963; Von Backström, 1962; Von Backström et al., 1953). More recently, Anhaeusser and Walraven (1999) employed field, petrological, geochemical, isotopic and geophysical data to determine the possible nature and extent of the various granitoid components beneath the blanketing cover sequences. Assisted by a limited number of single-grain Pb-evaporation dates on zircons from some of the granitoid samples these authors presented an episodic evolutionary model for the development of the Archaean basement in the region.

The purpose of this paper is to present new single zircon U-Pb geochronology for some of the most representative granitoid rocks described by Anhaeusser and Walraven (1999) and is aimed at better constraining the timing of the episodic granitoid emplacement model previously proposed. For this purpose, two dating techniques have been employed:

(1) conventional U-Pb dating of single zircon grains; and

(2) U-Th-Pb SHRIMP I and II analyses of selected zircons. The results are used to reassess the geochronological evolution of the Amalia-Kraaipan granitic terrane in the western sector of the Kaapvaal Craton.

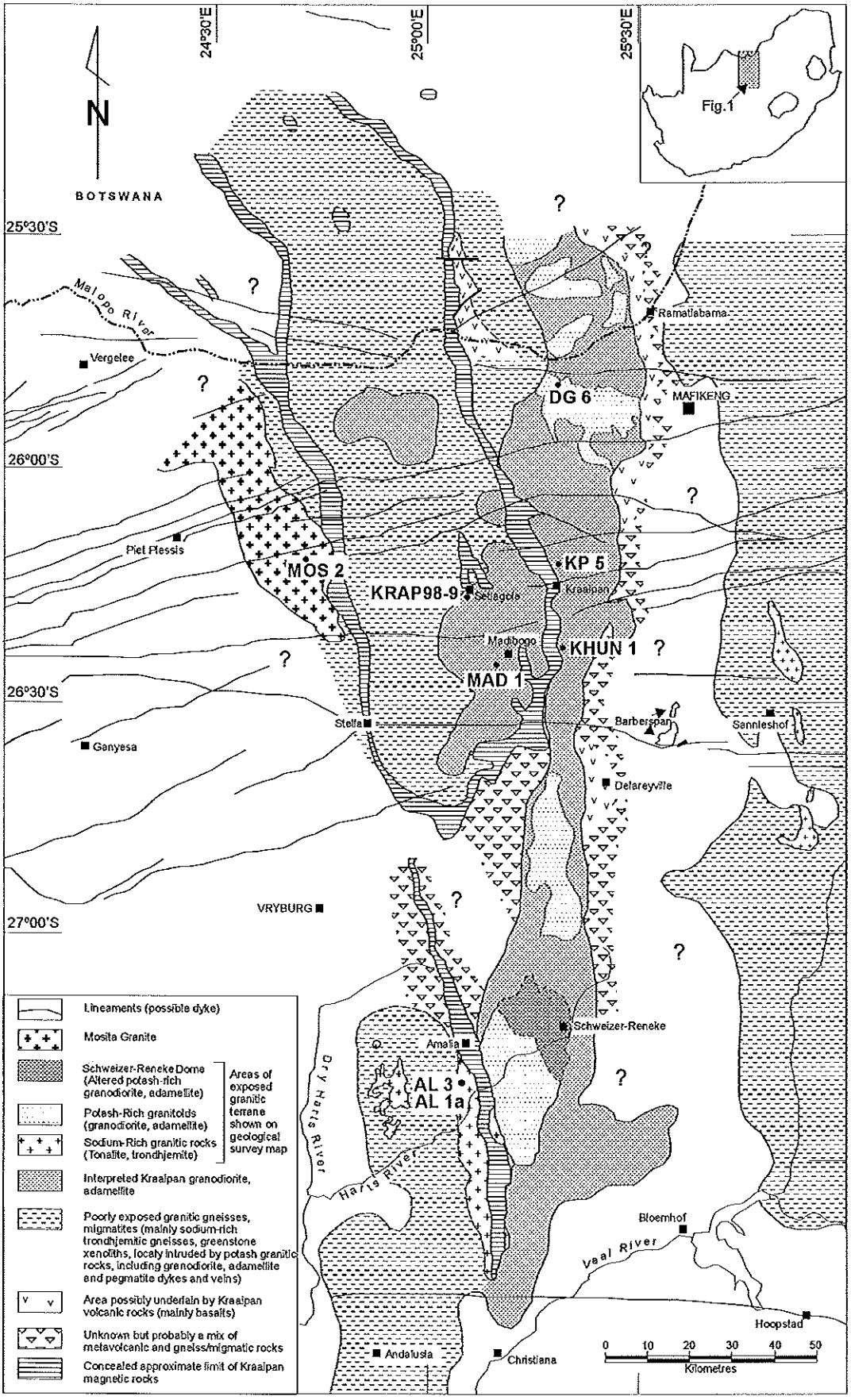

Figure 1: The Amalia-Kraaipan granite-greenstone terrane; combined field, aeromagnetic and gravity interpretation (after Anhaeusser and Walraven, 1999).

GENERAL GEOLOGY

The Kraaipan Group, consisting of metamorphosed volcano-sedimentary rocks and associated granitoids, occurs on the western margin of the Kaapvaal Craton and crops out sporadically from Botswana in the north to the Amalia - Schweizer-Reneke - Christiana areas in the south (Fig.1), a distance of approximately 250km. Basement granitoid rocks continue southwards for at least a further 150km where they are exposed in some of the diamond mines in the Kimberley and Koffiefontein areas. Zircon U-Pb ion microprobe (SHRIMP) ages ranging from *c.* 3250 – 2940 Ma were reported by Drennan et al. (1990) from samples of gneisses and migmatites from the Bultfontein Mine south of Kimberley.

Anhaeusser and Walraven (1999) described the Kraaipan granite-greenstone terrane in terms of a northern and a southern domain, separated by over 70 km of Ventersdorp Supergroup volcanic rocks, the latter blanketing the Archaean basement between Amalia and Schweizer – Reneke in the south and Delareyville in the north. The Kraaipan rocks in the northern domain occur in three, narrow, approximately north-south trending belts, which are separated by a variety of granitic, gneissic and migmatitic rocks. Only one belt, the Amalia greenstone belt, occurs in the southern domain. Sporadic greenstone occurrences have, however, been recorded in exposures west of the Amalia belt (Van Eeden et al., 1963; Liebenberg, 1977; Schutte, 1994) and in borehole intersections east of the belt (south of Schweizer-Reneke, T. R. Marshall, Gold Fields Ltd; pers. comm., 1991).

The volcanic rocks of the Kraaipan Group consist mainly of metamorphosed and hydrothermally altered, in places pillowed, tholeiitic and andesitic basalts and tuffs. These rocks now consist largely of altered to massive and schistose amphibolites and amphibole-chlorite-epidote schists. Banded iron formations (magnetite quartzites, banded ferruginous cherts, jaspilites, and iron formation breccias) are the main Archaean rock types exposed throughout the Amalia-Kraaipan region and are locally intensely deformed and contain gold – sulphide mineralization in places. Other rock types encountered in the greenstone successions include rare serpentinites, carbonate rocks, agglomerates, accretionary lapilli tuffs, conglomerates, grits, shales and phyllitic metasediments (Du Toit, 1906; Van Eeden et al., 1963; Jones and Anhaeusser, 1993; Zimmermann, 1994).

Despite the extensive cover of Tertiary to Recent Kalahari Group sediments, including wind blown sand, a variety of granitic rocks are exposed sporadically throughout the region. Most of the granitoid rocks crop out in river channels or poorly defined watercourses in the generally flattish terrain. Granitic rocks were also encountered in water storage pits, trenches, boreholes and, rarely, as flat whaleback pavement exposures. At least three varieties of granitoid rocks were recognised in the Kraaipan granite-greenstone terrane by previous workers associated with the Geological Surveys of South Africa and Botswana (Du Toit, 1906, 1908; SACS, 1980; Aldiss, 1985; Zimmermann, 1994). However, no regional synthesis or map showing the nature and distribution of the granite types had ever been attempted.

Anhaeusser and Walraven (1999) confirmed the three-fold classification of the granites on the basis of their distinctive petrological, geochemical and isotopic characteristics and, supported by aeromagnetic and Bouger gravity data, prepared a map showing their regional distribution (Fig.1). The various granitoid rocks, include: (1) foliated leucogneisses and migmatites (tonalitic and trondhjemitic gneisses) containing xenoliths of Kraaipan amphibolites and banded iron formations (outcropping localities widely dispersed from the Botswana border in the north to Amalia in the south); (2) fine-to medium-grained grey or

pink, homogeneous or, in places, weakly foliated, massive granitoids as well as cross-cutting dykes and vein (Kraaipan - Schweizer-Reneke granodiorite-adamellite suite); and (3) coarse-grained, homogeneous, pink granite (Mosita adamellite).

The tonalitic and trondhjemitic gneisses were regarded by Anhaeusser and Walraven (1999) as the earliest granitoids and yielded minimum single-grain zircon Pb evaporation ages ranging from 3162 to 3070 Ma. The potassium-enriched granodiorite-adamellite suite ranged in age from 2880 to 2846 Ma, whereas the Mosita adamellite yielded a Pb evaporation age of approximately 2749 Ma and represented the youngest intrusive body in the Kraaipan granite-greenstone terrane. A more detailed account of the previous geochronological findings are provided below.

Field and geophysical evidence (aeromagnetic and Bouguer gravity data), together with petrological, geochemical and isotopic data provided the basis for the compilation of a regional geological map for the Kraaipan granite-greenstone terrane (see Fig. 1). An evolutionary model of crustal development was proposed suggesting that the north-south trending Kraaipan volcano-sedimentary greenstone succession and the associated granitoid rocks may have accreted episodically on to the western edge of the Kaapvaal Craton during the time period extending from approximately 3250 to 2700 Ma.

PREVIOUS GEOCHRONOLOGICAL INVESTIGATIONS

Very few geochronological data are available for the Amalia-Kraaipan region. A summary of published ages and their interpretation is provided in Table 1. The oldest age reported so far for the basement gneisses (*c.* 3250 Ma) is from zircon cores extracted from a tonalitic gneiss from the Bultfontein diamond mine in the Kimberley area (Drennan et al., 1990). The rims of these zircons gave an age of *c.* 2940 Ma, which has been interpreted as a metamorphic age. Zircon evaporation data from borehole DKT, drilled approximately 9km west of Setlagole (Fig. 1), yielded ages of 3162 ± 8 Ma and 3070 ± 7 Ma, respectively, and have been interpreted as minimum ages for the crystallization (Anhaeusser and Walraven, 1999). A sample of gneiss-migmatite from borehole TA2 in the Schweizer-Reneke vicinity was dated at 2927 +23/-6 (Robb et al., 1992). This age has been interpreted as representative of a migmatization event which can be correlated with the *c.* 2940 Ma metamorphism recorded by zircon overgrowths in similar rocks from the Kimberley area (see above).

Several ages are available for the Schweizer-Reneke adamellite. They range between 2700 ± 55 Ma (Allsopp, 1964) and 2880 ± 2 Ma (see Table 1), the latter result being considered as the best estimate for the age of the Schweizer-Reneke adamellite. Hydrothermal veins cross-cutting the suite of tonalitic gneisses and migmatites that were, in turn, intruded by the Schweizer-Reneke adamellite have been dated at 2884 ± 2 Ma (Robb et al., 1992) leading to the conclusion that these veins represent an exogeneous hydrothermal manifestation of the Schweizer-Reneke granitoid intrusion.

Further north, zircons from the Kraaipan granodiorite, which Anhaeusser and Walraven (1999) correlated with the Schweizer-Reneke adamellite/granodiorite, yielded model evaporation ages ranging from 2790±2 to 2846±22 Ma with a weighted mean of 2805±9 Ma.

The Mosita adamellite, which is exposed in the northwestern part of the Amalia-Kraaipan terrane (Fig.1), represents the youngest granitoid event in the region, yielding ages of 2718 ±

65 Ma (Burger and Walraven, 1979) and 2749 ± 3 Ma (Anhaeusser and Walraven, 1999). The Mosita igneous event may possibly represent the last stages of plutonism linked to the emplacement, at approximately 2784 Ma, of the Gaberone Granite Suite and Kanye Formation on the northwestern edge of the Kaapvaal Craton described by Sibiya (1988), Grobler and Walraven (1993) and Moore et al. (1992, 1993). More recently, Grobler (1996) referred to these rocks as the Gaborone-Kanye igneous terrane.

Table 1. Summary and interpretation of previous isotopic data from the Amalia-Kraaipan granite-greenstone terrane

Sample Unit	Technique	Age in Ma	Interpretation	Reference
Schweizer-Reneke adamellite	Rb-Sr whole rock	2700±55	Age of crystallization	(3)
Mosita adamellite (MCH)	U-Pb (zircon population)	2718±65 (1σ)	Age of crystallization	(2)
Mosita adamellite (FW92 105)	Zircon evaporation	2749±3 (2σ)	Age of crystallization	(1)
Schweizer-Reneke adamellite	Rb-Sr whole rock	2767±120	Age of crystallization	(4)
Schweizer-Reneke adamellite	Pb-Pb whole rock	2780±70	Age of crystallization	(4)
Gaborone Granite Complex	Zircon evaporation	2781±2 (2σ)	Age of crystallization	(7)
Kraaipan Granodiorite (FW88 409)	Zircon evaporation	2846±22 (2σ)	Age of crystallization (?)	(1)
Schweizer-Reneke adamellite (TKB2)	U-Pb monazite	2880±2	Age of crystallization	(6)
Veins (TA2)	U-Pb rutile	2884±2 (2σ)	Age of hydrothermal event	(6)
Gneisses-migmatites (TA2)	U-Pb zircon	2927+23/-6 (2σ)	Age of migmatization (?)	(6)
Gneisses from Kimberley area	SHRIMP U-Pb zircon	2940 (rims)	Metamorphic overgrowths	(5)
Gneisses from Kimberley area	SHRIMP U-Pb zircon	3250 (cores)	(?)	(5)
Setlagole borehole DKT (FW92 104)	Zircon evaporation	From 2816±16 to 3070±7 (2σ)	Minimum and maximum for crystallization and disturbance ages, respectively	(1)
Setlagole borehole DKT (FW92 103)	Zircon evaporation	From 2866±25 to 3162±8 (2σ)	Minimum and maximum for crystallization and disturbance ages, respectively	(1)

(1): Anhaeusser and Walraven, 1999, (2): Burger and Walraven, 1979, (3): Allsopp, 1964, (4): Barton et al., 1986, (5): Drennan et al., 1990, (6): Robb et al., 1992, (7): Globler and Walraven, 1993.

Sampling

All the granitoid samples presented in this paper were described and classified by Anhaeusser and Walraven (1999) according to their K_2O and Na_2O contents (Fig. 2).

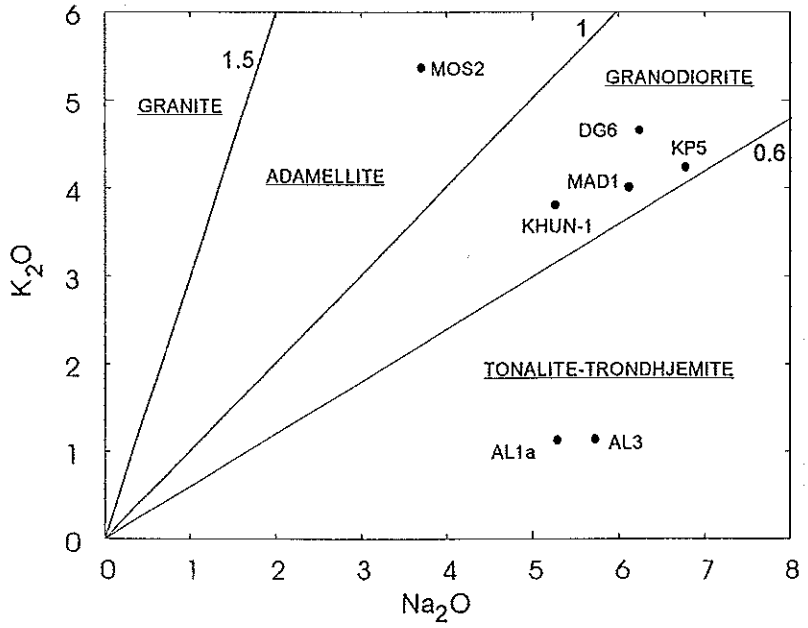

Figure 2: Plot of K_2O versus Na_2O for samples of Archaean granitoid basement rocks used in this isotopic study and listed in Tables 2 and 3. Original geochemical data from Anhaeusser and Walraven (1999).

Samples AL1a and AL3 (Fig.1) are from a small TTG granitoid platform cropping out approximately 7km south of Amalia. Sample AL1a is representative of a coarse-grained trondhjemite gneiss containing conformably interlayered amphibolite xenoliths (Fig.3A). A finer-grained, leuco-trondhjemitic gneissic phase, represented by sample AL3 (Fig.3B), occurs as dykes that are both conformable as well as transgressive to the coarser-grained gneisses. The TTG gneisses (AL1a and AL3) are regarded as representive of the earliest gneissic basement in the southern part of the Amalia-Kraaipan terrane. The amphibolite xenoliths, in turn, are considered to represent remnants of the Kraaipan metavolcanic succession of the Amalia greenstone belt, outcrops of which are located approximately 500m to the east of the granitoid platform.

Further to the north, representative samples of the pinkish-grey, homogeneous granodiorite/adamellite suite were sampled in the Madibogo-Kraaipan areas (Fig.1). Sample MAD1, a grey, medium-grained, homogeneous granodiorite was collected near the grain elevators in the Madibogo township and a jointed, brecciated and hydrothermally altered pinkish-grey granodiorite, displaying evidence of brittle deformation, was sampled in a river section near Khunwana (KHUN1; Fig.1). Sample KP5 was collected near the Kraaipan railway siding and consists of a homogeneous, pink, fine-to medium-grained granodiorite. Further to the north a sample of fine-grained, homogeneous, pinkish-grey granodiorite was collected on the eastern side of the Disaneng Dam (DG6, Fig.1). Finally, a much coarser-grained adamellite (MOS2, Fig.1) was sampled in a north-trending riverbed on the farm Mosita, approximately 40 km west of Setlagole.

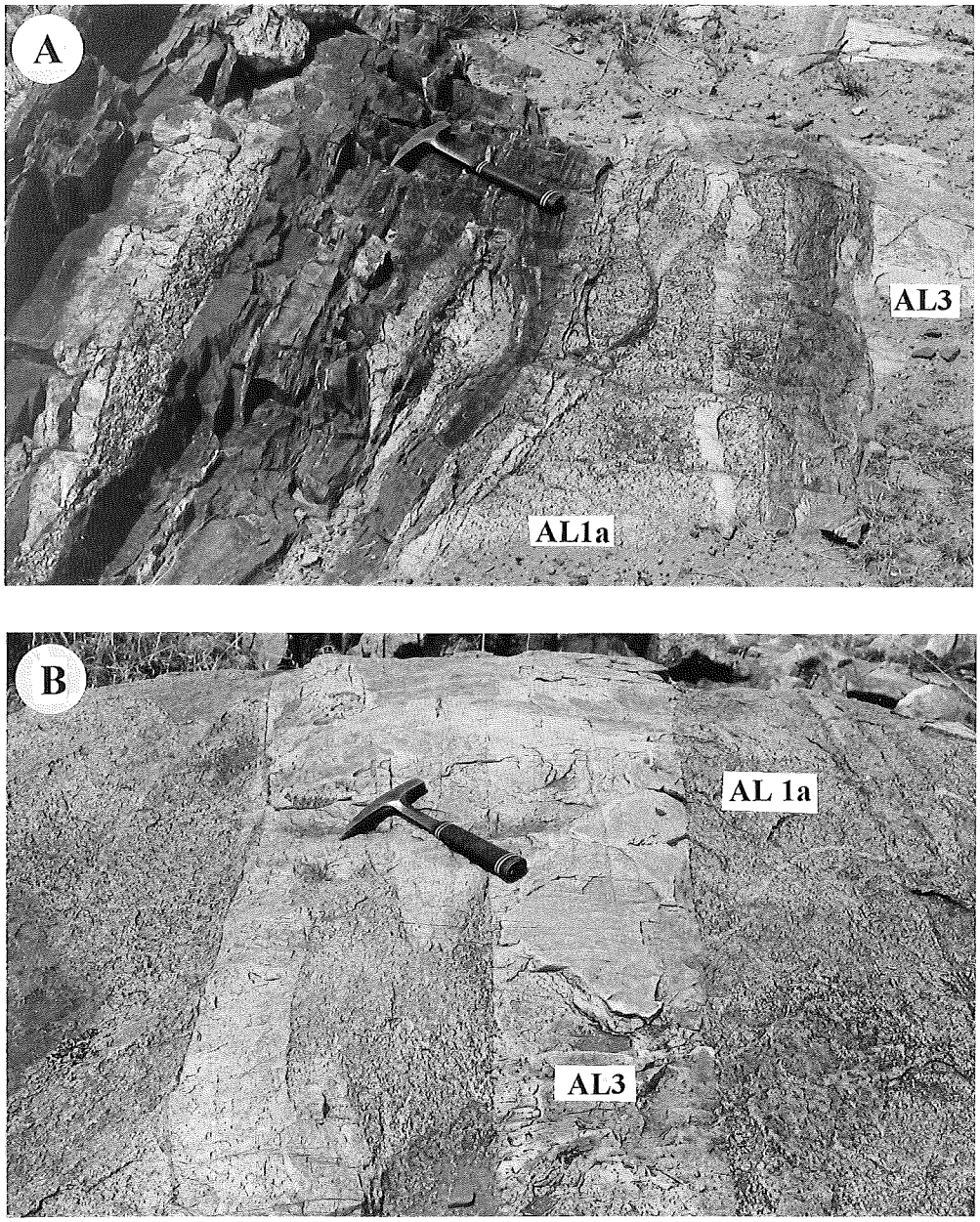

Figure 3: *Granite-greenstone pavement exposures located approximately 7 km south of Amalia on the farm Eerstbegin 99. (A). Hornblende-amphibolite xenolith conformably interlayered with trondhjemitic gneiss and intruded by fine-grained leuco-trondhjemitic dykes. (B). Coarse-grained trondhjemite gneiss (AL1a) intruded by leuco-trondhjemite dykes (AL3).*

ANALYTICAL TECHNIQUES

Mineral separates were prepared from 4-6kg rock samples at the in the Hugh Allsopp Laboratory, University of the Witwatersrand, Johannesburg. Rock samples were pulverized using a heavy-duty hydraulic rock splitter, jaw crusher and swing mill. Mineral separation involved the use of a Wilfley Table, heavy liquids (bromoform and methylene iodide) and a Frantz Isodynamic Separator.

U-Th-Pb SHRIMP I and II Analyses

Analyses were performed at the Research School for Earth Sciences (RSES) at the National Australian University, Canberra. Zircons were handpicked, mounted in epoxy and polished. Normal transmitted and reflected light microscopy, as well as SEM cathodoluminescence imagery, was used to determine the internal structures of the zircons prior to analysis. Data were collected and reduced as described by Williams and Claesson (1987) and Compston et al. (1992). U/Pb ratios were referenced to the RSES standard zircon AS3 standard (1099.1 Ma, $^{206*}Pb/^{238}U$=0.1859, Paces and Miller, 1989). U and Th concentrations were determined relative to those measured in the RSES zircon standard SL13. All errors quoted in Table 2 are listed at 1σ, but where data are combined for regression analysis or to calculate weighted means, the final result is quoted with 95% confidence limits. All the geochronological statistical assessments were performed using the Isoplot/Ex program of Ludwig (2000).

U-Pb Conventional Single Zircon Technique

Analyses were performed at the Hugh Allsopp Laboratory, University of the Witwatersrand. Zircons were examined with a binocular microscope in order to assess grain quality, degree of fracturing and the possible existence of inherited cores. Handpicked zircons were abraded using the techniques of Krogh (1982) and washed in ultra-pure acetone, diluted nitric acid and hydrochloric acid. Single grains or small populations of zircons were then placed into 0.35 ml Teflon vials together with 30 µl HF and a mixed ^{205}Pb-^{235}U spike. Eight of these Teflon vials were placed in a Parr Container for 2 days at 220°C. The samples were chemically processed without separating U and Pb (Lancelot et al., 1976) and loaded on a rhenium filament together with a 0.25N phosphoric acid - silica-gel mixture. The analyses were performed on an automated VG54E mass spectrometer using a Daly collector and corrected by 0.12%/AMU for thermal mass fractionation. Total Pb blanks over the period of the analyses range from 15 to 30 pg and a value of 30pg was assigned as the laboratory blank ($^{206}Pb/^{204}Pb$=18.97 ± 1, $^{207}Pb/^{204}Pb$=15.73 ± 0.5 and $^{208}Pb/^{204}Pb$=39.19 ± 1.5). The calculation of common Pb was made by subtracting blanks and then assuming that the remaining common Pb has been incorporated into the crystal and has a composition determined from the model of Stacey and Kramers (1978). Data were reduced using PbDat (Ludwig, 1993a). Analytical uncertainties in Table 3 are listed at 2σ and age determinations were processed using Isoplot/Ex (Ludwig, 2000).

RESULTS AND INTERPRETATIONS

Trondhjemitic Granitoid Samples

Sample AL1a is a trondhjemitic gneiss associated with amphibolite xenoliths (Fig.3). Zircons extracted from this sample were generally pink in colour and translucent. Some zircons, however, presented some possible overgrowths. A total of 12 single zircon grains were analyzed and the data is listed in Table 3. U and Pb contents are highly variable, ranging from 12 to 545 ppm and 29 to 303 ppm, respectively. Plotted on a concordia diagram (Fig.4A), the data do not define a simple, single group or trend and clearly any age calculation is complicated by the probable presence of more than one age population. This initially heterogeneous age population is further complicated by variable discordance and the effects of more than one Pb-loss event. In our interpretation of the data we do, however, recognise two ages defined by the combination of data points that appear to conform to discrete

concordia trends. The first age is defined by four zircon analyses (Zr 2, 4, 5, 7, Fig.4A), which may be regressed to give a well-constrained upper intercept age of 3008±4 Ma (MSWD = 0.57) with a lower intercept of 69 ± 37 Ma. Three zircons (Zr 6, 8, 9, Fig. 4A) define an upper intercept age of 2859 ± 4 Ma (MSWD = 0.54). One zircon (Zr 1) is perfectly concordant at 3050 ± 35 Ma. The remaining zircons plot between the 2.86 Ga and the 3.01 Ga discordias (Fig. 4A).

Sample AL3 is from a leuco-trondhjemite dyke intruded into the coarser-grained trondhjemite gneiss (sample AL1a). Zircons extracted from this sample were pink in colour. Cathodoluminescence imaging of these zircons shows that they are compositionally zoned displaying cores and overgrowths (Fig. 5). Twenty spots from 15 different zircons were analyzed on SHRIMP II and the data are reported in Table 2. Ten analyses which plot as a group on, or within error of, concordia combine to give a weighted mean $^{207}Pb/^{206}Pb$ age of 2939 ± 9.6 Ma (MSWD = 2.7), which we consider to be the most reliable estimate of the age of emplacement of the leuco-trondhjemite dykes. As with the previous sample, the Pb-loss history of the more discordant analyses is not simple. All the analyses but three (6.1, 12.1 and 14.1) can be regressed with the concordant group described above to define an upper intercept age of 2943 ± 14 Ma (MSWD = 1.4) and a lower intercept age of 1252 ± 59 Ma. This Pb-loss history could be a consequence of the later thermal events recorded in the other samples analysed from the area and discussed in the section that follows. In the broader regional context, one such event, which could have had such an influence, was the *c.* 1200 Ma metamorphism and magmatism of the Namaqua-Natal Mobile Belt, which wraps around the western margin of the Kaapvaal Craton.

Although many grains appear to be structured into apparent cores and overgrowths some of these are clearly indistinguishable and probably represent growth under different conditions, but within the same crystallization event. In Figure 5 grain 14 is such an example, where the core and rim have the same $^{207}Pb/^{206}Pb$ ages within error, but have very different Th/U compositions (Table 2). Other core/overgrowth structures are clearly recording very different events. The core analysis 15.1 (Fig.5) yields a concordant $^{207}Pb/^{206}Pb$ age of 2920 ± 18 Ma while the overgrowth (15.2) defines a discordant $^{207}Pb/^{206}Pb$ minimum age of 2120 ± 15 Ma. The highly discordant nature of the rim analysis does, unfortunately, make it difficult to define the age of this overgrowth with any accuracy or confidence. One grain (12.1, Fig. 5) has a core with a measured $^{207}Pb/^{206}Pb$ 93% concordant age of 3178 ± 10 Ma and clearly represents an inherited zircon from the pre-existing basement.

In the light of the data obtained from sample AL1a and sample AL3, we can distinguish 3 main events. The first event, defined by zircons from sample AL1a at 3008 ± 4 Ma, we consider to be the age of the emplacement of the TTG granitoids in this region. Older ages at 3178 and 3050 Ma, respectively (Zr1 and grain spot 12.1), represent xenocrysts inherited from the older granite-greenstone material or from the source from which the granitoids were derived. A second event, corresponding to the intrusion of the leuco-trondhjemite AL3 within the TTG suite, took place at 2939 ± 9.6 Ma as defined by the concordant zircons from sample AL3. This age can be compared to the age of 2927 +23/-6 Ma found by Robb et al. (1992) for a TTG sample in the Schweizer-Reneke vicinity (Fig. 1; Table 1). Discordant analyses from samples AL1a and AL3 (Fig.4A and 4B, solid line), which give apparent $^{207}Pb/^{206}Pb$ ages of about 2860 Ma could also be recording this event, viz. the emplacement of the nearby Schweizer-Reneke granite dated by Robb et al., (1992) at 2880 Ma (Table 1). However, there is no field (e.g. veining), petrographic (e.g. zircon overgrowths) nor geochemical (e.g. low Th/U zircons) evidence to support new zircon growth at this time. These $^{207}Pb/^{206}Pb$ apparent ages are most likely recording a complex post-crystallization Pb-loss history.

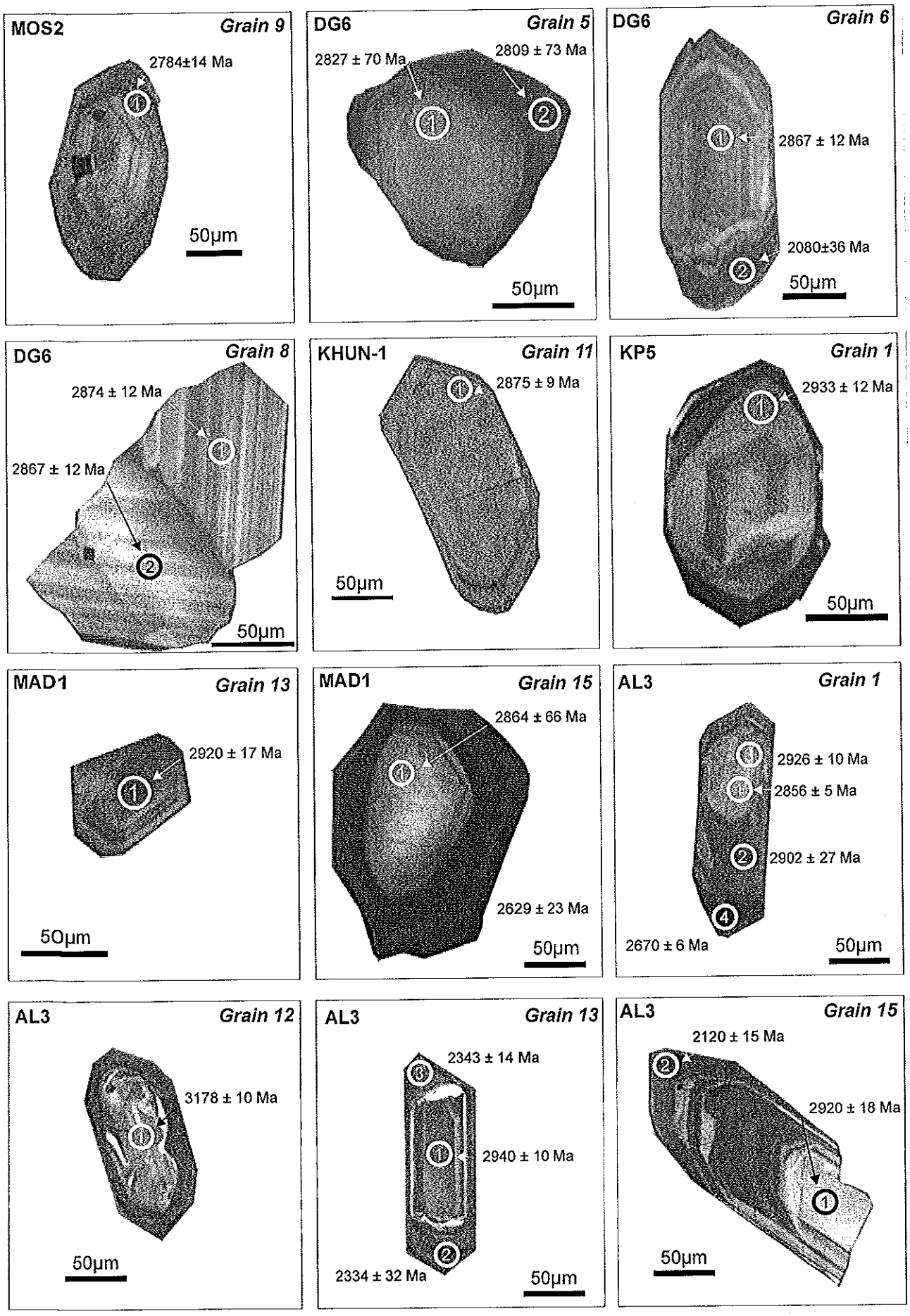

Figure 5: *Cathodoluminescence photographs showing the internal structure of some of the zircons analysed from samples MOS2, DG6, KHUN1, KP5, MAD1 and AL3.*

Table 2. SHRIMP U-Pb analyses

Grain. spot	U (ppm)	Th (ppm)	Th/U	$^{204}Pb/^{206}Pb$	Pb* (ppm)	Radiogenic Ratios						Ages (In Ma)						Conc. %
						$^{206}Pb/^{238}U$	±	$^{207}Pb/^{235}U$	±	$^{207}Pb/^{206}Pb$	±	$^{206}Pb/^{238}U$	±	$^{207}Pb/^{235}U$	±	$^{207}Pb/^{206}Pb$	±	
Sample MOS2																		
1.1	42	60	1.43	0.00018	31	0.5415	0.021	14.711	0.61	0.1970	0.002	2790	89	2797	40	2802	18	100
2.1	86	80	0.93	0.00000	59	0.5477	0.017	14.798	0.47	0.1960	0.001	2816	70	2802	31	2793	11	101
3.1	122	118	0.97	0.00020	79	0.5185	0.015	14.062	0.42	0.1967	0.001	2693	64	2754	29	2799	9	96
4.1	129	104	0.81	0.00012	87	0.5520	0.016	14.989	0.46	0.1970	0.001	2833	68	2815	29	2801	9	101
5.1	124	391	3.15	0.00532	92	0.5615	0.017	15.188	0.60	0.1962	0.005	2873	69	2827	38	2795	38	103
6.1	139	326	2.35	0.00277	71	0.3784	0.012	10.330	0.40	0.1980	0.004	2069	55	2465	37	2810	33	74
7.1	104	102	0.98	0.00054	72	0.5552	0.017	14.910	0.51	0.1948	0.002	2847	72	2810	33	2783	19	102
8.1	141	103	0.73	0.00003	83	0.4950	0.015	13.220	0.41	0.1937	0.001	2592	64	2696	30	2774	10	94
9.1	67	68	1.00	0.00004	48	0.5638	0.016	15.152	0.45	0.1949	0.002	2882	65	2825	29	2784	14	104
10.1	111	105	0.95	0.00067	61	0.4403	0.015	12.029	0.44	0.1982	0.002	2352	66	2607	35	2811	17	84
11.1	146	115	0.78	0.00164	79	0.4241	0.012	11.622	0.39	0.1987	0.003	2279	56	2574	32	2816	23	81
12.1	130	191	1.47	0.00419	66	0.3763	0.013	9.961	0.51	0.1920	0.006	2059	63	2431	49	2759	56	75
13.1	294	705	2.40	0.01201	159	0.3832	0.014	9.923	0.50	0.1878	0.006	2091	66	2428	47	2723	49	77
14.1	91	72	0.80	0.00018	64	0.5784	0.016	15.457	0.45	0.1938	0.002	2942	64	2844	28	2775	13	106
Sample DG6																		
1.1	101	83	0.83	0.00030	63	0.502	0.022	14.465	0.64	0.2088	0.001	2624	93	2781	43	2896	11	91
2.1	169	64	0.38	0.00209	70	0.331	0.006	9.353	0.19	0.2046	0.002	1846	27	2373	19	2864	15	65
3.1	64	52	0.81	0.00005	48	0.603	0.012	17.203	0.39	0.2068	0.002	3044	49	2946	22	2880	13	106
4.1	104	82	0.79	0.00000	69	0.542	0.016	15.472	0.51	0.2070	0.002	2793	69	2845	32	2882	15	97
5.1	74	48	0.65	0.00262	51	0.554	0.015	15.288	0.81	0.2001	0.008	2842	64	2833	52	2827	70	101
5.2	8598	680	0.08	0.03172	1512	0.086	0.004	2.356	0.16	0.1979	0.009	534	24	1229	49	2809	73	19
6.1	237	222	0.94	0.00014	171	0.569	0.016	16.095	0.49	0.2050	0.001	2905	67	2882	29	2867	12	101
6.2	2365	1651	0.70	0.00651	530	0.180	0.005	3.199	0.12	0.1287	0.003	1069	29	1457	30	2080	36	51
7.1	43	28	0.64	0.00024	31	0.597	0.022	17.157	0.68	0.2083	0.002	3019	89	2944	39	2893	17	104
8.1	84	76	0.91	0.00000	62	0.590	0.017	16.755	0.50	0.2060	0.002	2989	68	2921	29	2874	12	104
8.2	53	41	0.77	0.00011	37	0.571	0.016	16.136	0.48	0.2051	0.002	2911	64	2885	29	2867	14	102
9.1	92	102	1.12	0.00284	56	0.490	0.015	13.363	0.74	0.1979	0.008	2569	64	2706	53	2809	71	92
10.1	93	73	0.78	0.00029	65	0.565	0.018	16.117	0.55	0.2069	0.002	2887	76	2884	33	2881	12	100
11.1	141	184	1.31	0.00046	86	0.464	0.014	13.315	0.42	0.2080	0.002	2458	61	2702	31	2890	14	85
12.1	84	51	0.60	0.00243	51	0.491	0.014	13.588	0.47	0.2009	0.003	2573	61	2721	33	2833	27	91
Sample KHUN-1																		
1.1	911	853	0.94	0.00020	227	0.2101	0.003	3.425	0.06	0.1183	0.001	1229	18	1510	14	1930	10	64
2.1	483	197	0.41	0.00030	266	0.4881	0.009	13.532	0.26	0.2011	0.001	2562	39	2718	18	2835	7	90
3.1	317	185	0.58	0.00214	128	0.3428	0.006	8.657	0.20	0.1832	0.002	1900	30	2303	21	2682	21	71
4.1	721	84	0.12	0.00760	226	0.2757	0.007	6.404	0.21	0.1684	0.002	1570	37	2033	29	2542	25	62
5.1	237	93	0.39	0.00003	153	0.5702	0.015	16.356	0.43	0.2081	0.001	2909	60	2898	25	2891	5	101
6.1	203	73	0.36	0.00003	136	0.5980	0.011	17.232	0.34	0.2090	0.001	3022	46	2948	19	2898	5	104
7.1	574	205	0.36	0.00015	293	0.4632	0.007	11.624	0.19	0.1820	0.001	2454	33	2575	16	2671	5	92
8.1	222	57	0.26	0.00025	138	0.5630	0.010	15.877	0.31	0.2045	0.001	2879	43	2869	19	2863	7	101
9.1	304	90	0.30	0.00092	193	0.5636	0.010	16.187	0.30	0.2083	0.001	2882	41	2888	18	2892	8	100
10.1	164	41	0.25	0.00024	101	0.5575	0.010	15.855	0.30	0.2063	0.001	2856	40	2868	18	2877	8	99
11.1	176	62	0.35	0.00035	108	0.5393	0.010	15.319	0.30	0.2060	0.001	2781	41	2835	19	2875	9	97
12.1	278	100	0.36	0.00013	172	0.5535	0.010	15.543	0.29	0.2037	0.001	2840	41	2849	18	2856	5	99
13.1	116	38	0.32	0.00040	74	0.5734	0.011	16.347	0.33	0.2068	0.001	2922	44	2897	20	2880	10	101
14.1	209	394	1.88	0.01354	94	0.3136	0.010	7.760	0.65	0.1800	0.013	1758	48	2206	78	2653	127	66
15.1	80	48	0.60	0.00012	56	0.5897	0.011	16.742	0.33	0.2059	0.001	2988	44	2920	19	2874	9	104
Sample KP5																		
1.1	52	20	0.39	0.59690	35	0.2136	0.002	17.580	0.58	0.2136	0.002	3017	75	2987	32	2933	12	103
2.1	268	467	1.74	0.47930	171	0.2113	0.002	13.965	0.33	0.2113	0.002	2524	45	2747	22	2916	12	87
3.1	224	285	1.27	0.53270	152	0.2143	0.003	15.739	0.45	0.2143	0.003	2753	51	2861	28	2938	25	94
4.1	267	242	0.91	0.40320	130	0.2078	0.002	11.553	0.27	0.2078	0.002	2184	38	2569	22	2889	13	76
5.1	113	177	1.57	0.59140	79	0.2105	0.001	17.163	0.40	0.2105	0.001	2995	53	2944	23	2909	8	103
6.1	373	222	0.60	0.26140	126	0.2035	0.003	7.333	0.26	0.2035	0.003	1497	41	2153	33	2854	24	53
7.1	347	266	0.77	0.39560	160	0.2075	0.003	11.318	0.38	0.2075	0.003	2149	50	2550	32	2886	26	75
8.1	219	171	0.78	0.49000	129	0.2093	0.001	14.138	0.32	0.2093	0.001	2571	45	2759	22	2900	10	89
9.1	332	359	1.08	0.44510	169	0.2076	0.002	12.737	0.28	0.2076	0.002	2373	40	2660	21	2887	13	82
10.1	314	646	2.06	0.31840	131	0.2005	0.003	8.802	0.30	0.2005	0.003	1782	47	2318	31	2830	21	63
11.1	384	87	0.23	0.32840	143	0.1902	0.002	8.610	0.23	0.1902	0.002	1831	35	2298	24	2744	20	67
12.1	160	164	1.03	0.56350	113	0.2105	0.001	16.354	0.37	0.2105	0.001	2881	50	2898	22	2909	9	99
13.1	183	358	1.95	0.59530	134	0.2097	0.001	17.212	0.39	0.2097	0.001	3011	50	2947	22	2903	11	104
14.1	405	369	0.91	0.29080	151	0.1923	0.002	7.711	0.23	0.1923	0.002	1646	39	2198	27	2762	17	60
15.1	534	145	0.27	0.31380	182	0.1655	0.003	7.162	0.24	0.1655	0.003	1759	41	2132	30	2513	28	70
Sample MAD1																		
1.1	498	706	1.42	0.02836	429	0.5313	0.008	13.731	0.35	0.1874	0.004	2747	33	2731	24	2720	31	101
2.1	152	103	0.68	0.00048	102	0.5574	0.011	16.007	0.38	0.2083	0.002	2856	48	2877	23	2892	15	99
3.1	332	337	1.02	0.01240	149	0.3339	0.006	9.265	0.32	0.2013	0.006	1857	30	2365	33	2837	46	66
4.1	598	495	0.83	0.00078	272	0.3826	0.006	8.754	0.15	0.1659	0.001	2089	28	2313	16	2517	7	83
5.1	781	636	0.81	0.02625	944	0.7805	0.011	20.342	0.42	0.1890	0.003	3719	41	3108	20	2734	22	136

Table 2 (Contd.)

Grain, spot	U (ppm)	Th (ppm)	Th/U	$^{204}Pb/^{206}Pb$	Pb* (ppm)	Radiogenic Ratios $^{206}Pb/^{238}U$	±	$^{207}Pb/^{235}U$	±	$^{207}Pb/^{206}Pb$	±	Ages (in Ma) $^{206}Pb/^{238}U$	±	$^{207}Pb/^{235}U$	±	$^{207}Pb/^{206}Pb$	±	Conc. %
6.1	280	90	0.32	0.00311	146	0.4519	0.007	12.590	0.24	0.2021	0.002	2404	33	2650	18	2843	14	85
7.1	166	103	0.62	0.00014	112	0.5671	0.011	16.483	0.36	0.2108	0.001	2896	47	2905	21	2912	10	100
8.1	120	52	0.43	0.00005	80	0.5776	0.011	16.909	0.34	0.2123	0.001	2939	45	2930	19	2923	7	101
9.1	90	72	0.80	0.00076	61	0.5530	0.011	16.201	0.36	0.2125	0.002	2838	45	2889	21	2925	14	97
10.1	87	65	0.75	0.00017	62	0.5817	0.014	16.919	0.43	0.2109	0.001	2956	55	2930	24	2913	12	102
11.1	297	91	0.31	0.00224	168	0.4958	0.010	14.158	0.33	0.2071	0.002	2596	42	2760	22	2883	16	90
12.1	177	187	1.05	0.00283	90	0.4105	0.007	11.512	0.29	0.2034	0.003	2217	33	2566	24	2853	26	78
13.1	151	69	0.46	0.00171	93	0.5282	0.009	15.434	0.33	0.2119	0.002	2734	39	2842	21	2920	17	94
14.1	40	51	1.28	0.00326	25	0.4948	0.015	14.713	0.56	0.2157	0.004	2591	64	2797	37	2949	33	88
15.1	48	73	1.54	0.01430	22	0.3565	0.009	10.063	0.49	0.2047	0.008	1966	41	2441	46	2864	66	69
15.2	1126	216	0.19	0.02716	631	0.3540	0.007	8.658	0.22	0.1774	0.002	1954	33	2303	23	2629	23	74
Sample AL3																		
1.1	507	320	0.63	0.00027	292	0.4818	0.008	13.528	0.24	0.2037	0.001	2535	35	2717	17	2856	5	89
1.2	355	178	0.50	0.00018	164	0.5222	0.015	15.09	0.50	0.2096	0.003	2709	69	2821	31	2902	27	91
1.3	124	40	0.32	0.00022	58	0.5411	0.016	15.66	0.48	0.2126	0.001	2788	69	2864	28	2926	10	94
1.4	445	55	0.12	0.00019	164	0.4212	0.012	10.56	0.30	0.1818	0.001	2266	57	2485	24	2670	6	82
2.1	387	85	0.22	0.00015	201	0.4798	0.008	13.093	0.22	0.1979	0.001	2526	35	2686	16	2809	5	90
3.1	134	37	0.27	0.00025	87	0.5829	0.011	17.330	0.37	0.2156	0.002	2961	45	2953	21	2948	13	100
4.1	256	62	0.24	0.00008	166	0.5833	0.012	17.384	0.37	0.2162	0.001	2962	50	2956	21	2952	4	100
5.1	348	160	0.46	0.00093	213	0.5338	0.009	15.279	0.28	0.2076	0.001	2758	39	2833	18	2887	7	96
6.1	301	342	1.14	0.00620	149	0.4348	0.007	12.637	0.27	0.2108	0.003	2327	32	2653	21	2912	20	80
7.1	319	113	0.36	0.00016	202	0.5604	0.009	16.413	0.27	0.2124	0.001	2868	37	2901	16	2924	5	98
8.1	209	67	0.32	0.00023	133	0.5681	0.011	16.854	0.34	0.2152	0.001	2900	43	2927	19	2945	9	99
9.1	614	185	0.30	0.00042	239	0.3584	0.006	8.332	0.14	0.1686	0.001	1975	27	2268	16	2544	8	78
10.1	92	30	0.32	0.00043	58	0.5672	0.021	16.706	0.66	0.2136	0.002	2896	87	2918	38	2933	16	99
11.1	329	107	0.32	0.00044	190	0.5207	0.009	14.562	0.27	0.2028	0.001	2702	38	2787	17	2849	7	95
12.1	123	68	0.55	0.00101	85	0.5780	0.010	19.837	0.38	0.2489	0.001	2941	42	3083	19	3178	10	93
13.1	213	52	0.24	0.00049	138	0.5851	0.009	17.303	0.31	0.2145	0.001	2969	39	2952	17	2940	10	101
13.2	629	84	0.13	0.00056	184	0.3211	0.009	6.60	0.23	0.1490	0.003	1795	49	2059	23	2334	32	68
13.3	894	21	0.02	0.00065	258	0.3231	0.009	6.67	0.20	0.1498	0.001	1805	47	2069	20	2343	14	70
14.1	151	28	0.19	0.00388	36	0.2228	0.005	6.434	0.19	0.2094	0.004	1297	24	2037	27	2901	32	45
14.2	160	1	0.01	0.00018	94	0.5658	0.013	16.639	0.40	0.2133	0.001	2891	53	2914	24	2931	10	99
15.1	41	14	0.35	0.00057	27	0.5805	0.012	16.962	0.41	0.2119	0.002	2951	47	2933	23	2920	18	101
15.2	998	212	0.21	0.00149	279	0.2691	0.004	4.884	0.09	0.1316	0.001	1536	20	1800	15	2120	15	73

Table 3: U-Pb data (conventional technique) for sample AL1a

Grain	Weight µg	U (ppm)	Pb* (ppm)	$^{204}Pb/^{206}Pb$	Radiogenic Ratios $^{206}Pb/^{238}U$	± (%)	$^{207}Pb/^{235}U$	± (%)	$^{207}Pb/^{206}Pb$	± (%)	Ages (in Ma) $^{206}Pb/^{238}U$	±	$^{207}Pb/^{235}U$	±	$^{207}Pb/^{206}Pb$	±	Conc. %
Zr 1	12	12	29	0.00752	0.6085	1.6	19.269	2.0	0.2297	1.1	3064	50	3055	60	3050	35	100
Zr 2	10	73	43	0.00279	0.4588	3.4	14.052	3.5	0.2222	0.6	2434	83	2753	96	2996	18	81
Zr 3	14	73	32	0.00177	0.3480	0.9	10.200	1.0	0.2126	0.4	1925	16	2453	24	2925	13	66
Zr 4	10	151	59	0.00124	0.3160	1.9	9.636	2.1	0.2212	0.7	1770	34	2401	51	2989	21	59
Zr 5	10	43	31	0.00523	0.5516	0.7	17.000	0.8	0.2235	0.3	2832	21	2935	23	3006	10	94
Zr 6	6	423	239	0.00087	0.5350	1.0	15.043	1.1	0.2039	0.4	2762	27	2818	30	2858	10	97
Zr 7	6	58	44	0.00108	0.6009	2.6	18.551	2.6	0.2239	0.3	3034	79	3019	79	3009	9	101
Zr 8	4	29	18	0.00694	0.5131	3.4	14.527	4.9	0.2053	3.0	2670	91	2785	136	2869	85	93
Zr 9	5	545	303	0.00048	0.5178	2.7	14.583	2.7	0.2043	0.4	2690	73	2788	76	2861	11	94
Zr 10	6	153	94	0.00135	0.5149	1.0	15.348	1.1	0.2162	0.2	2678	28	2837	30	2953	7	91
Zr 11	6	103	58	0.00027	0.5287	1.7	15.299	1.7	0.2099	0.1	2736	48	2834	49	2905	2	94
Zr 12	6	79	85	0.00130	0.5238	1.2	15.437	1.3	0.2138	0.6	2715	33	2843	38	2934	17	93

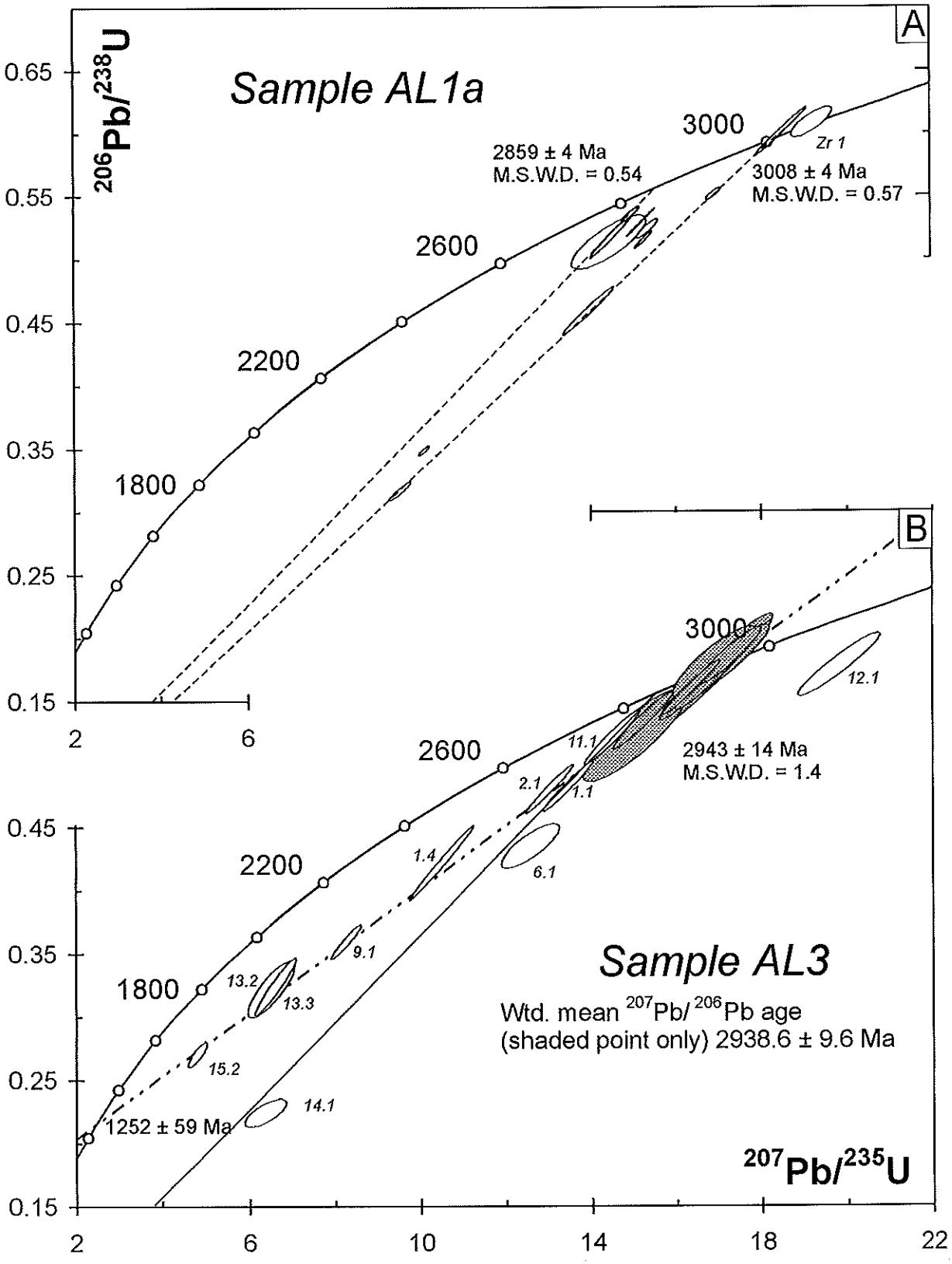

Figure 4: *(A) Conventional technique U-Pb concordia diagram of single zircons from sample AL1a. Only the shaded ellipses have been used for data regressions; (B) SHRIMP II concordia diagram for sample AL3. Only the shaded ellipses have been used for the weighted-mean calculation. The dashed lines in both plots represent the discordia ages calculated from the sample data. Solid lines are the discordia reported from the other sample. All data-point error ellipses and listed ages are at 95% confidence levels.*

Granodiorites and Adamellites

Zircons extracted from sample KP5 are compositionally zoned, prismatic grains, with a typical darker rim (Fig. 5). Fifteen spots, corresponding to 15 zircon grains, were analyzed with SHRIMP II (Table 2). Plotted in a concordia diagram (Fig. 6A) the analyses show highly variable discordance. A weighted mean $^{207}Pb/^{206}Pb$ mean age calculated for the more than 90% concordant points gives 2913 ± 15 Ma (MSWD = 1.2). An upper intercept age calculated for all the analyses bar 15.1 gives a similar age at 2919 ± 19 Ma (MSWD = 3.6).

Zircons from sample MAD1 are also compositionally zoned with some of them possessing a large darker rim (Fig. 5). Sixteen grain spots, corresponding to 15 grains, have been analyzed with SHRIMP II (Table 2). Their positions in a concordia diagram (Fig. 6B) range between concordant to discordant. A weighted mean $^{207}Pb/^{206}Pb$ age calculated from the more concordant analyses (>90% concordant) gives an age of 2917 ± 9Ma (n=6; MSWD = 0.86). Upper and lower intercept ages of 2917 ± 10 Ma and 457 ± 150 Ma (MSWD = 2) can be calculated by regression of 13 of the data points (Fig.6B). Some of the zircons from this sample are highly discordant and/or do not fall on this discordia. Discordance appears to be unrelated to U content (e.g. the two analyses from grain 15, which have vastly different U contents of 48 and 1126 ppm and yet show similar discordance). Another interesting aspect of the zircon geochemistry of the sample is the extremely high common Pb content (over 30% of $_{206}$) of some zircons. Clearly these zircons have been influenced by a post-emplacement event which has affected some of the zircons quite significantly leading in one case (5.1) to anomalous reverse discordance. It is possible that the timing of this event is given by the analysis 1.1, which gives a $^{207}Pb/^{206}Pb$ age of 2720 ± 31 Ma and is within error of concordia. This age is geologically significant in the area as it is similar to the age of the Ventersdorp Supergroup volcanics (Armstrong et al., 1991) which cover most of this region. The extreme (>37% of $_{206}$) common Pb content of this zircon, however, must make this analysis suspect and it is unlikely that this zircon has maintained its isotopic integrity.

Therefore, samples KP5 and MAD1 yield identical ages at, respectively, 2913 ± 17 Ma and 2917 ± 9 Ma thereby defining a magmatic event in the Kraaipan vicinity at *c.* 2.92 Ga.

Zircons from sample DG6 are typically prismatic, compositionally zoned and present exceptionally darker rims under cathodoluminescence (Fig. 5). Fifteen spots have been analyzed with SHRIMP I (Table 2). Of these 15 analyses, 12 are concordant and define a weighted $^{207}Pb/^{206}Pb$ mean age of 2879 ± 9 Ma (Fig. 7) considered as the emplacement age for this granodiorite. An upper intercept age can be calculated at 2878 ± 8 Ma (MSWD = 0.77) for these 12 spots together with spots 2.1 and 5.2 (Fig. 5). The spot analyses 5.2 and 6.2 (Fig. 5) revealed very high uranium and lead contents. These uranium-rich rims were clearly susceptible to weathering and post-crystallisation alteration during younger events as is demonstrated by their very discordant positions in the diagram (Fig. 7).

All the zircons extracted from sample KHUN1 are prismatic with a very discreet zonation (Fig. 5). Fifteen grain-spot analyses were performed with SHRIMP I (Table 2). A total of 9 concordant grains define a weighted $^{207}Pb/^{206}Pb$ mean age of 2879 ± 11 Ma considered as the emplacement age for this granodiorite. Several spots give younger apparent $^{207}Pb/^{206}Pb$ ages indicating intermediate and complex Pb-loss.

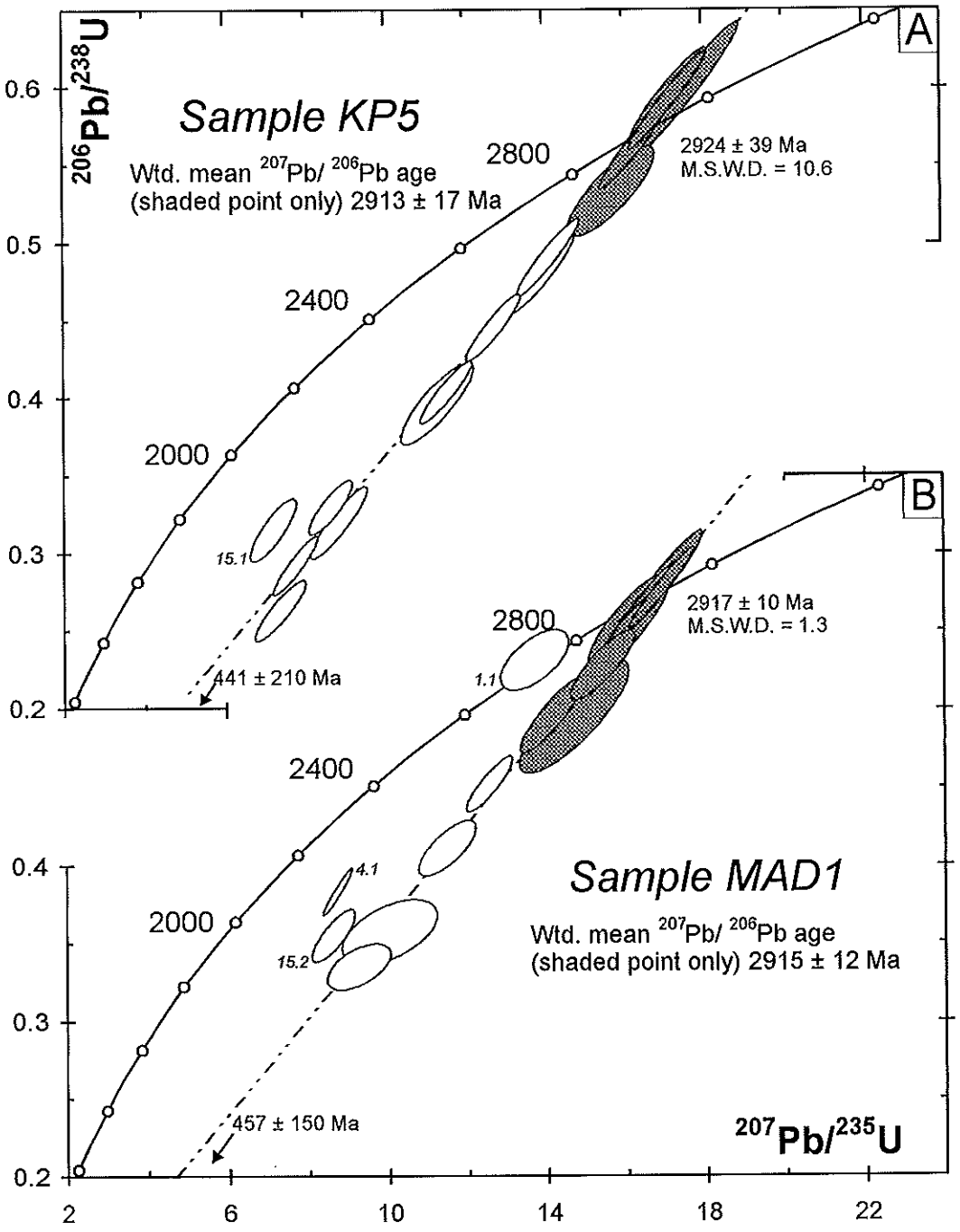

Figure 6: Concordia diagram showing SHRIMP II analyses of granodiorite samples KP5 (A) and MAD1 (B). Data-point error ellipses are at 1σ (68.3%) confidence levels while calculated ages are at 2σ (95%) confidence levels.

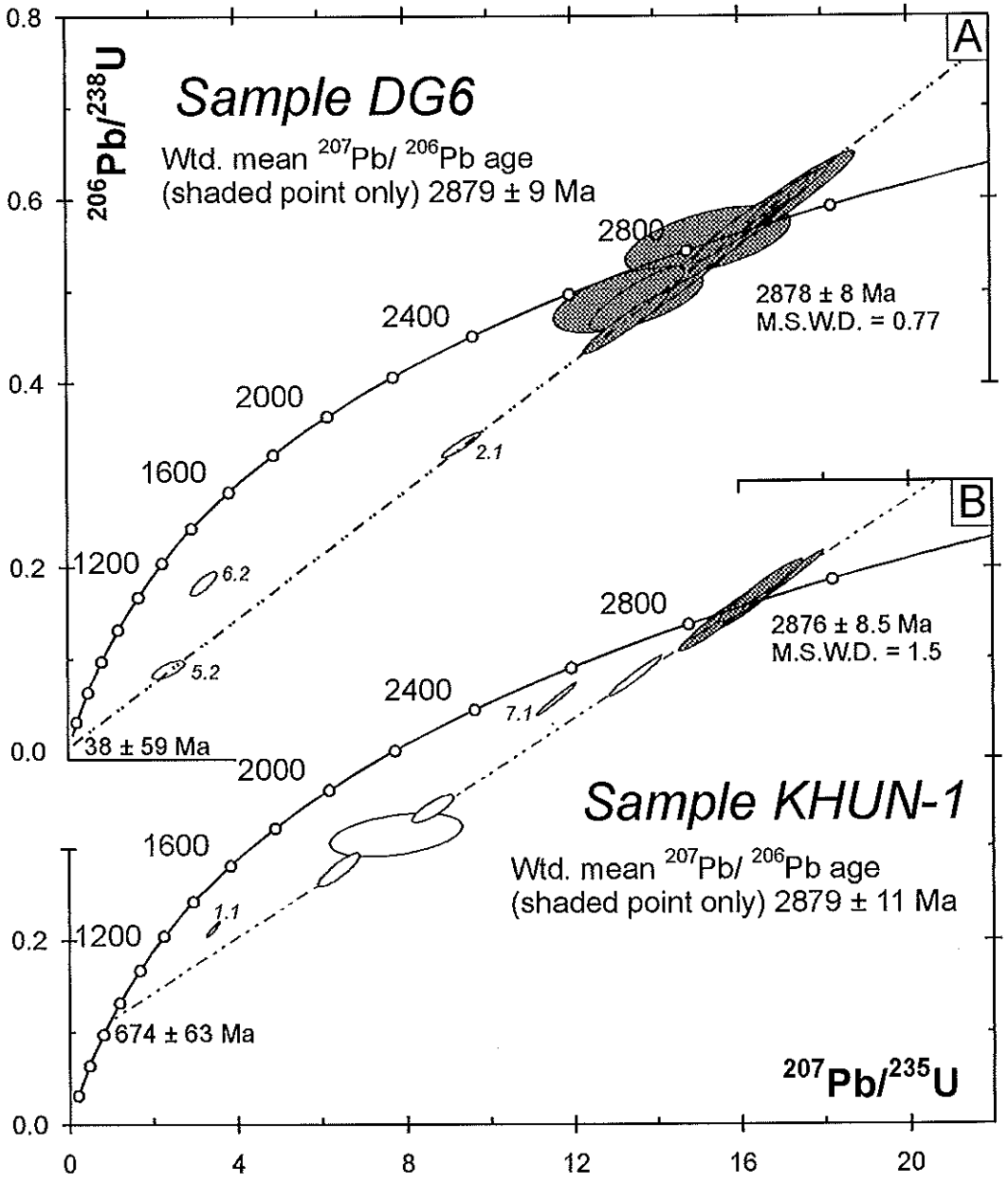

Figure 7: Concordia diagram showing SHRIMP I analyses for granodiorite samples DG6 (A) and KHUN-1 (B). Data-point error ellipses are at 1σ (68.3%) confidence levels while calculated ages are at 2σ (95%) confidence levels.

Ages found for samples DG6 and KHUN1 are indistinguishable at 2879 ± 9 Ma and 2879 ± 11 Ma respectively, defining a magmatic event both in the central and northern parts of the Amalia-Kraaipan terrane at *c.* 2880 Ma. This age is identitical to the age of 2880 Ma found by Robb et al. (1992) for the Schweizer-Reneke granite further to the south.

The adamellite MOS2 provided a very homogeneous zircon population characterized by prismatic shapes, concentric compositional magmatic zonation and rare inclusions (Fig.5). Fourteen spots were analyzed with SHRIMP I (Table 2). Plotted on a concordia diagram (Fig.8) all the data define a well-constrained upper intercept age at 2791 ± 8 Ma (MSWD = 0.94) with a lower intercept age at 56 ± 230 Ma. The weighted $^{207}Pb/^{206}Pb$ mean age for the

more than 90% concordant grains define an identical age at 2790 ± 8 Ma, considered as the emplacement age for the Mosita adamellite.

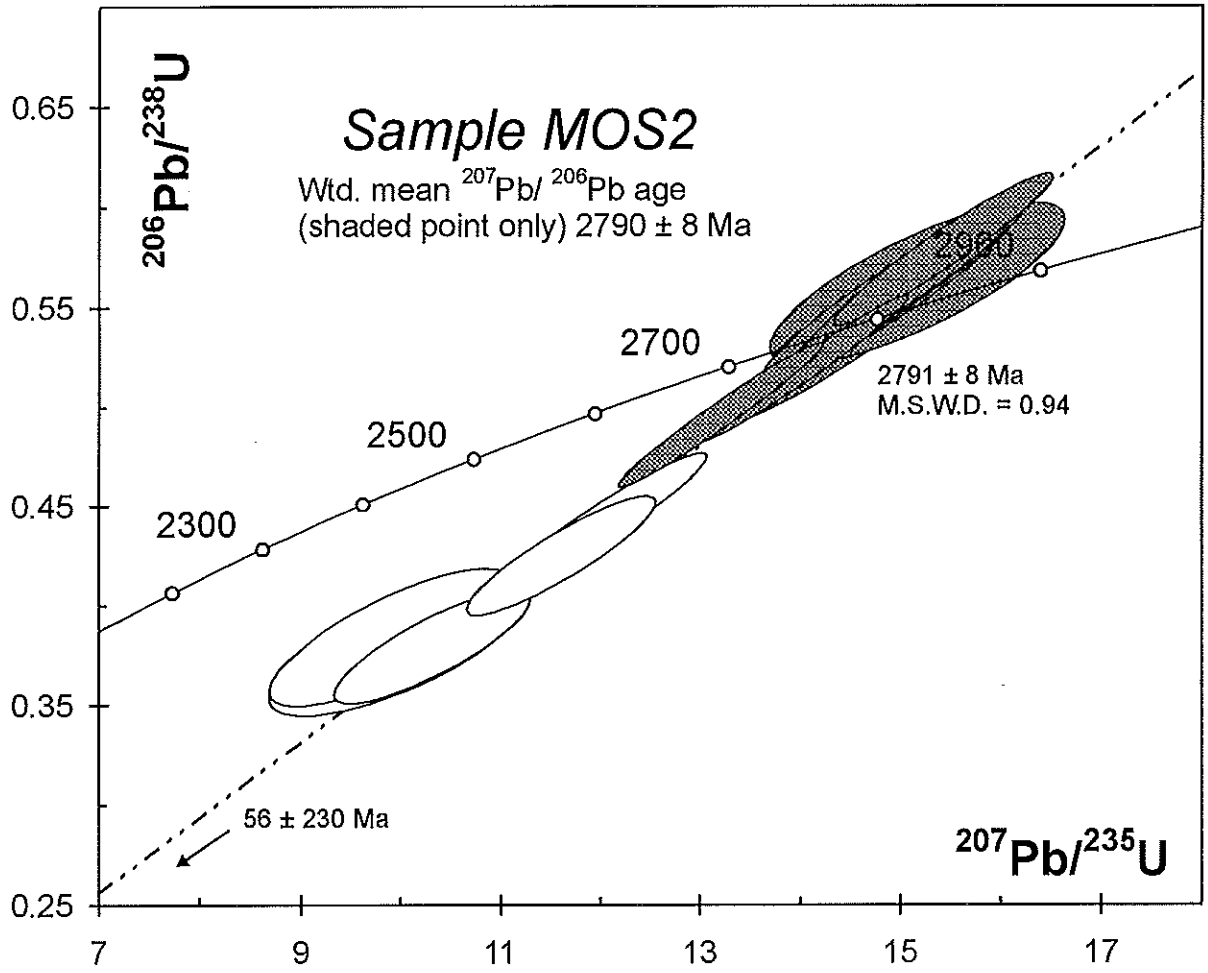

Figure 8: Concordia diagram showing SHRIMP I analyses for the coarse-grained Mosita adamellite sample MOS2. Data-point error ellipses are at 1σ (68.3%) confidence levels while calculated ages are at 2σ (95%) confidence levels.

CONCLUSIONS

The new U-Pb data presented in this paper demonstrates the episodic emplacement of granitoid rocks in the Amalia-Kraaipan terrane over a period of *c.* 250 Ma. A trondhjemitic gneiss from the Kraaipan basement in the vicinity of the town of Amalia has been dated at *c.* 3008 Ma. This gneiss was, in turn, intruded by a leuco-trondhjemitic dyke event at *c.* 2940 Ma. It is interesting to note that an age of *c.* 1250 Ma was also found for this sample (lower intercept). This implies that these rocks were possibly influenced by the Namaqua-Natal orogeny that occurred at approximately this time further to the south.

Two granodiorite samples collected in the central part of the Amalia-Kraaipan terrane were dated at 2913 ± 17 Ma and 2915 ± 12 Ma, respectively, and two other granodiorites from both the central and northern part of the study area were dated at 2879 ± 9 Ma and 2879 ± 11 Ma. Finally, the Mosita adamellite, cropping out in the northwest of the Amalia-Kraaipan terrane was dated at 2791 ± 8 Ma.

The Amalia-Kraaipan terrane is defined by a TTG gneiss-migmatite assemblage with numerous amphibolite and, in places, banded iron formation xenoliths related to the Kraaipan Group (Anhaeusser and Walraven, 1999), the latter intruded by a variety of granitoids. As the TTG component has been shown to be 3008 Ma years old in the Amalia region, the volcano-sedimentary rocks of the Kraaipan Group must, therefore, be older than 3008 Ma. The true age of the Kraaipan Group might be further constrained by the older zircons (at 3050 Ma and 3178 Ma) found in the gneissic trondhjemites and the leuco-trondhjemite dykes. A second magmatic event took place between 2940 Ma and 2920 Ma. This event was also identified by Robb et al. (1992) for a *c.* 2930 Ma old suite of TTG gneisses intruded by the Schweizer-Reneke granite in the southern part of the study area. A third major magmatic event, identified throughout the north-south extent of the Amalia-Kraaipan terrane, took place at *c.* 2880 Ma. The granitoids associated with this event are believed to have played an important role in controlling gold mineralization in the region. Anhaeusser and Walraven (1999) pointed out that all the known gold deposits south of Amalia (Goudplaats, Abelskop, Bothmansrust) as well as in the region north of Kraaipan (Kalahari Goldridge, Madibe) occur in the greenstone successions adjacent to the *c.* 2880 Ma granitoids. Finally, the Mosita adamellite was emplaced at *c.* 2790 Ma. This age approximates the age of 2780 Ma found for the Gaborone Granite Suite and Kanye Formation in the area north of Mafikeng (Grobler and Walraven, 1993; Grobler, 1996). It is therefore suggested that the Mosita granitoid body may represent part of a major, more widespread, magmatic and volcanic event that occurred on the northwestern edge of the Kaapvaal Craton at *c.* 2790 Ma.

In conclusion, the magmatic history of the Amalia-Kraaipan terrane is defined by episodic granitoid emplacement over a period of approximately 220 Ma. The Witwatersrand Basin, the western margin of which is situated only 60 km to the east of this granite-greenstone basement, was deposited between 3074 and 2714 Ma (Armstrong et al., 1991). The source area of the Witwatersrand Basin (more specifically the western goldfields, Robb et al., 1992), was thought to be largely made up of ~3200-2900 Ma old rocks (Barton et al., 1989; Robb et al., 1990; Poujol et al., 1999) located somewhere along the western margin of the Kaapvaal Craton. The *c.* 3010 to 2920 Ma Amalia-Kraaipan granitoids could, therefore, represent a component of the source terrane for the Witwatersrand sediments and the Kraaipan volcano-sedimentary rocks the source of some of the Witwatersrand gold mineralization. Furthermore, the present data supports the suggestions by Robb et al. (1992) that mineralization in the Witwatersrand Basin took place as a consequence of the intrusion of numerous granitoid bodies in close proximity to the Witwatersrand Basin preceding and during its deposition. This study confirms that enormous quantities of granitoid rocks were emplaced between 3010 and 2790 Ma in the western hinterland of the Witwatersrand Basin during a time span closely overlapping the 3074 to 2714 Ma ages determined for the basin deposition.

REFERENCES

Aldiss, D. T., 1985. The geology of the Phitsane area. Explanation of Sheets 2525C and 2525D, Botswana. Bulletin, Geological Survey of Botswana, **28**, 106pp.

Allsopp, H. L., 1964. Rubidium/strontium ages of the Western Transvaal. Nature, **204**: 361-362.

Anhaeusser, C. R., 1973. The geology and geochemistry of the Archaean granites and gneisses of the Johannesburg and Pretoria dome. Special Publication of the Geological Society of South Africa, **3**: 361-385.

Anhaeusser, C. R., 1999. Archaean crustal evolution of the central Kaapvaal Craton, South Africa: evidence from the Johannesburg Dome. South African Journal of Geology, **102** (4):303-322.

Anhaeusser, C. R. and Burger, A. J., 1982. An interpretation of U-Pb zircon ages for Archaean tonalitic gneisses from the Johannesburg-Pretoria granite dome. Transactions of the Geological Society of South Africa, **85**: 111-116.

Anhaeusser, C. R. and Walraven, F., 1999. Episodic granitoid emplacement in the western Kaapvaal Craton: evidence from the Archaean Kraaipan granite-greenstone terrane, South Africa. Journal of African Earth Sciences, **28** (2): 289-309.

Armstrong, R. A., Compston, W., Retief, E.A., Williams, I. S. and Welke, H. J., 1991. Zircon ion microprobe studies bearing on the age and evolution of the Witwatersrand triad. Precambrian Research, **53**: 243-266.

Barton, E. S., Barton, J. M. Jr., Callow, M. J., Allsopp, H. L., Evans, I. B. and Welke, H. J., 1986. Emplacement ages and implications for the source region of granitoid rocks associated with the Witwatersrand Basin. Extended Abstract, Geocongress '86, Johannesburg, pp. 93-97.

Barton, E. S., Compston, W., Williams, I. S., Bristow, J. W., Hallbauer, D. K. and Smith, C., 1989. Provenance ages for the Witwatersrand Supergroup and the Ventersdorp Contact Reef: contraints from ion microprobe U-Pb ages of detrital zircons. Economic Geology, **84**: 2012-2019.

Burger, A. J. and Walraven, F., 1979. Summary of age determinations carried out during the period April 1977 to March 1978. Annals of the Geological Survey of South Africa, **12**: 209-218.

Compston, W., Williams, I. S., Kirschvink, J. L., Zhang, Z. and Ma, G., 1992. Zircon U-Pb ages for the early Cambrian time-scale. Journal Geology Society of London, **149**(171-184).

Drennan, G. R., Robb, L. J., Meyer, F. M., Armstrong, R. A. and De Bruiyn, H., 1990. The nature of the Archaean basement in the hinterland of the Witwatersrand Basin: II. A crustal profile west of the Welkom Goldfield and comparisons with the Vredefort crustal profile. South African Journal of Geology, **93**: 41-53.

Du Toit, A. L., 1906. Geological survey of portions of the division of Vryburg and Mafeking. Annual report of the Geological Commission of the Cape of Good Hope (1905), 205-258.

Du Toit, A. L., 1908. Geological survey of portion of Mafeking and Vryburg. Annual Report of the Geological Commission of the Cape of Good Hope (1907), 123-157.

Grobler, D. F., 1996. The geology, geochemistry and geochronology of the Gaberone Granite Suite and Kanye Formation north of Mafikeng, South Africa. Ph.D thesis (unpubl.), University of the Witwatersrand, Johannesburg, 457pp.

Grobler, D. F. and Walraven, F., 1993. Geochronology of Gaborone Granite Complex extensions in the area north of Mafikeng, South Africa. Chemical Geology (Isotope Geoscience Section) **105**: 319-337.

Jones, I. M. and Anhaeusser, C. R., 1993. Accretionary lapilli associated with Archaean banded iron formations of the Kraaipan Group, Amalia greenstone belt, South Africa. Precambrian Research, **61**: 117-136.

Keyser, N. and Du Plessis, C. P., 1993. The geology of the Vryburg area. Explanation sheet 2624 (Vryburg). Geological Survey of South Africa, 28 pp.

Klemd, R. and Hallbauer, D. K., 1987. Hydrothermally altered peraluminous Archean granites as a provenance model for Witwatersrand sediments. Mineralium Deposita, **22**: 227-235.

Krogh, T. E., 1982. Improved accuracy of U-Pb ages by the creation of more concordant systems using an air abrasion technique. Geochimica et Cosmochimica Acta, **46**: 617-649.

Lancelot, J., Vitrac, A. and Allegre, C. J., 1976. Uranium and lead isotopic dating with grain by grain zircon analysis : a study of complex geological history with a single rock. Earth Planetary Sciences Letters, **29**: 357-366.

Lienbenberg, J., 1977. *Die geologie van die gebied 2724D (Andalusia).* M.Sc. thesis (unpubl.), University of the Orange Free State, Bloemfontein, 233 pp.

Ludwig, K.R., 1993. A computer program for processing Pb-U-Th isotope data, version 1.24, Denver. United States Geological Survey, Open File Report, 88-542: 32pp.

Ludwig, K. R., 2000. *Isoplot/Ex: a Geochronological Toolkit for Microsoft Excel.* Berkeley Geochronology Center, Berkeley, California.

Michaluk, E. and Moen, H. F. G., 1991. The geology of the Mafikeng area. Explanation sheet 2525 (Mafikeng). Geological Survey of South Africa, 44 pp.

Moore, M., Davis, D. W., Robb, L. J., Jackson, M. C. and Grobler, D. F., 1993. Archean rapakivi granite-anorthosite-rhyolite complex in the Witwatersrand Basin hinterland, southern Africa. Geology, **21**: 1031-1034.

Moore, M., Robb, L. J., Davis, D. W., Grobler, D. F. and Jackson, M. C., 1992. U-Pb zircon dates from an Archaean rapakivi granite-anorthosite-rhyolite complex in the Witwatersrand hinterland, southern Africa. Inform. Circ. Economic Geology Research Unit, University of the Witwatersrand, Johannesburg, **260**, 15pp.

Paces, J. B. and Miller Jr., J. D., 1989. Precise U-Pb ages of the Duluth Complex and related mafic intrusions, northeastern Minnesota: geochronological insights to physical, petrogenetic, paleomagnetic and tectonomagmatic processes associated with the 1.1 Ga mid-continent rift system. Journal of Geophysical Research, **B98**: 13997-14013.

Poujol, M. and Anhaeusser, C. R., (1999). The Johannesburg Dome, Kaapvaal Craton, South Africa, revisited in the light of new U-Pb single zircon dating. Inform. Circ. Economic Geology Research Institute, University of the Witwatersrand, Johannesburg, **339**, 15pp.

Poujol, M., Robb, L. J. and Respaut, J. P., 1999. U-Pb and Pb-Pb isotopic studies relating to the origin of gold mineralization in the Evander Goldfield, Witwatersrand Basin, South Africa. Precambrian Research, **95**:167-185.

Robb, L. J., Davis, D.W. and Kamo, L., 1990. U-Pb ages on single grain detrital zircon grains from the Witwarersrand Basin, South Africa : constraints on the age of sedimentation and the evolution of granites adjacent to the basin. Journal of Geology, **98**: 311-328.

Robb, L. J., Davis, D. W., Kamo, S. L. and Meyer, F. M., 1992. Ages of altered granites adjoining the Witwatersrand Basin with implications for the origin of gold and uranium. Nature, **357**: 677-680.

Robb, L. J. and Meyer, F. M., 1990. The nature of the Witwatersrand hinterland : Conjectures on the source area problem. Economic Geology, **85**: 511-536.

South African Committee for Stratigraphy (SACS), 1980. Stratigraphy of South Africa. Part 1. (Compiler, L. E. Kent). Lithostratigraphy of the Republic of South Africa, South West Africa / Namibia, and the Republics of Bophuthatswana, Transkei and Venda. Handbook, Geological Survey of South Africa, **8**, 690pp.

Schutte, I. C., 1994. Die geologie van die gebied Christiana. Explanation Sheet 2724 (Christiana). Geological Survey of South Africa, 58 pp.

Sibiya, V. B., 1988. The Gaberone Granite Complex, Botswana, southern Africa: an atypical rapakivi granite-massif anorthosite association. Free University Press, Amsterdam, 449pp.

Van Eeden, O. R., De Wet, N. P. and Strauss, C. A., 1963. The geology of the area around Schweizer-Reneke. An explanation of Sheets 2724B (Pudimoe) and 2725A (Schweizer-Reneke), Geological Survey of South Africa.

Von Backström, J. W., 1962. Die geologie van die gebied om Ottosdal, Transvaal. An explanation of Sheets 2625 D (Barberspan) and 2626 C (Ottosdal). Geological Survey of South Africa, 63 pp.

Von Backström, J. W., Schumann, F. W., Le Roex, H. D., Kent, L. E. and Du Toit, A. L., 1953. The geology of the area around Lichtenburg. Explanation Sheet 54 (Lichtenburg). Geological Survey of South Africa, 70 pp.

Williams, I. S. and Claesson, S., 1987. Isotopic evidence for the Precambrian provenance and Caledonian metamorphism of high grade paragneisses from the Seve Nappes, Scandinavian Caledonides. II. Ion microprobe zircon U-Th-Pb. Contributions to Mineralogy and Petrology, 97: 205-217.

Zimmermann, O. T., 1994. Aspects of the geology of the Kraaipan Group in the Northern Cape Province and the Republic of Bophuthatswana. M.Sc. dissertation, University of the Witwatersrand, Johannesburg, 145pp.

oOo